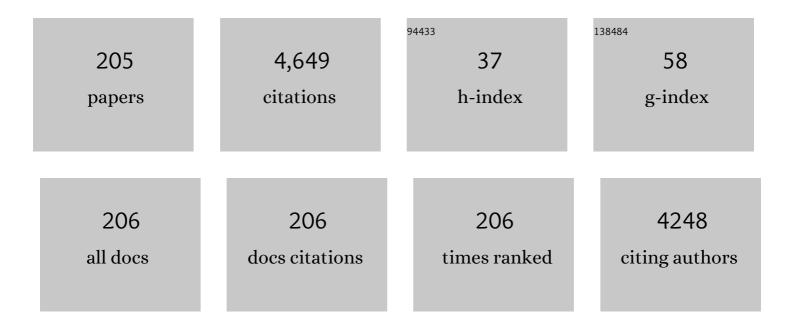
## Marina N Rumyantseva

List of Publications by Year in descending order

Source: https://exaly.com/author-pdf/4001737/publications.pdf Version: 2024-02-01



#	Article	IF	CITATIONS
1	Structural Characterization of Nanocrystalline SnO2by X-Ray and Raman Spectroscopy. Journal of Solid State Chemistry, 1998, 135, 78-85.	2.9	340
2	Raman Surface Vibration Modes in Nanocrystalline SnO2:  Correlation with Gas Sensor Performances. Chemistry of Materials, 2005, 17, 893-901.	6.7	162
3	Heterostructured p-CuO (nanoparticle)/n-SnO2 (nanowire) devices for selective H2S detection. Sensors and Actuators B: Chemical, 2013, 181, 130-135.	7.8	148
4	CuO/SnO2 thin film heterostructures as chemical sensors to H2S. Sensors and Actuators B: Chemical, 1998, 50, 186-193.	7.8	117
5	Nanocomposites SnO2/Fe2O3: Sensor and catalytic properties. Sensors and Actuators B: Chemical, 2006, 118, 208-214.	7.8	117
6	Reduced graphene oxide hybridized with WS2 nanoflakes based heterojunctions for selective ammonia sensors at room temperature. Sensors and Actuators B: Chemical, 2019, 282, 290-299.	7.8	112
7	Visible-light activated room temperature NO2 sensing of SnS2 nanosheets based chemiresistive sensors. Sensors and Actuators B: Chemical, 2020, 305, 127455.	7.8	109
8	Role of surface hydroxyl groups in promoting room temperature CO sensing by Pd-modified nanocrystalline SnO2. Journal of Solid State Chemistry, 2010, 183, 2389-2399.	2.9	81
9	Surface chemistry of nanocrystalline SnO2: Effect of thermal treatment and additives. Sensors and Actuators B: Chemical, 2007, 126, 52-55.	7.8	77
10	Nanocrystalline ZnO(Ga): Paramagnetic centers, surface acidity and gas sensor properties. Sensors and Actuators B: Chemical, 2013, 182, 555-564.	7.8	74
11	Chemical modification of nanocrystalline tin dioxide for selective gas sensors. Russian Chemical Reviews, 2013, 82, 917-941.	6.5	72
12	Dopants in nanocrystalline tin dioxide. Russian Chemical Bulletin, 2003, 52, 1217-1238.	1.5	68
13	Visible light activated room temperature gas sensors based on nanocrystalline ZnO sensitized with CdSe quantum dots. Sensors and Actuators B: Chemical, 2014, 205, 305-312.	7.8	68
14	The Key Role of Active Sites in the Development of Selective Metal Oxide Sensor Materials. Sensors, 2021, 21, 2554.	3.8	67
15	Nanocrystalline BaSnO3 as an Alternative Gas Sensor Material: Surface Reactivity and High Sensitivity to SO2. Materials, 2015, 8, 6437-6454.	2.9	63
16	Selective detection of individual gases and CO/H2 mixture at low concentrations in air by single semiconductor metal oxide sensors working in dynamic temperature mode. Sensors and Actuators B: Chemical, 2018, 254, 502-513.	7.8	61
17	One-dimensional CuO–SnO2 p–n heterojunctions for enhanced detection of H2S. Journal of Materials Chemistry A, 2013, 1, 11261.	10.3	58
18	Effect of combined Pd and Cu doping on microstructure, electrical and gas sensor properties of nanocrystalline tin dioxide. Materials Science and Engineering B: Solid-State Materials for Advanced Technology, 2001, 85, 43-49.	3.5	56

#	Article	IF	CITATIONS
19	Nanocomposites SnO2/Fe2O3: Wet chemical synthesis and nanostructure characterization. Sensors and Actuators B: Chemical, 2005, 109, 64-74.	7.8	55
20	UV effect on NO 2 sensing properties of nanocrystalline In 2 O 3. Sensors and Actuators B: Chemical, 2016, 231, 491-496.	7.8	54
21	Selectivity Modification of SnO <sub>2</sub> â€Based Materials for Gas Sensor Arrays. Electroanalysis, 2010, 22, 2809-2816.	2.9	53
22	Visible light activation of room temperature NO 2 gas sensors based on ZnO, SnO 2 and In 2 O 3 sensitized with CdSe quantum dots. Thin Solid Films, 2016, 618, 253-262.	1.8	53
23	Chemical modification of nanocrystalline metal oxides: effect of the real structure and surface chemistry on the sensor properties. Russian Chemical Bulletin, 2008, 57, 1106-1125.	1.5	51
24	Co3O4 as p-Type Material for CO Sensing in Humid Air. Sensors, 2017, 17, 2216.	3.8	51
25	Mechanism of sensing CO in nitrogen by nanocrystalline SnO2 and SnO2(Pd) studied by Mössbauer spectroscopy and conductance measurements. Journal of Materials Chemistry, 2002, 12, 1174-1178.	6.7	49
26	Nature of Gas Sensitivity in Nanocrystalline Metal Oxides. Russian Journal of Applied Chemistry, 2001, 74, 440-444.	0.5	47
27	Microstructure and electrophysical properties of SnO2, ZnO and In2O3 nanocrystalline films prepared by reactive magnetron sputtering. Materials Science and Engineering B: Solid-State Materials for Advanced Technology, 2002, 96, 268-274.	3.5	45
28	Nanocrystalline SnO2 and In2O3 as materials for gas sensors: The relationship between microstructure and oxygen chemisorption. Thin Solid Films, 2009, 518, 1283-1288.	1.8	44
29	A real-time on-line photoelectrochemical sensor toward chemical oxygen demand determination based on field-effect transistor using an extended gate with 3D TiO2 nanotube arrays. Sensors and Actuators B: Chemical, 2019, 289, 106-113.	7.8	44
30	Effect of interdiffusion on electrical and gas sensor properties of CuO/SnO2 heterostructure. Materials Science and Engineering B: Solid-State Materials for Advanced Technology, 1999, 57, 241-246.	3.5	43
31	SnO2/MoO3-nanostructure and alcohol detection. Sensors and Actuators B: Chemical, 2006, 118, 156-162.	7.8	42
32	Synthesis, Structure, and Sensor Properties of Vanadium Pentoxide Nanorods. European Journal of Inorganic Chemistry, 2010, 2010, 5247-5253.	2.0	42
33	Copper and nickel doping effect on interaction of SnO2 films with H2S. Journal of Materials Chemistry, 1997, 7, 1785-1790.	6.7	40
34	Oxygen exchange on nanocrystalline tin dioxide modified by palladium. Journal of Solid State Chemistry, 2012, 186, 1-8.	2.9	40
35	ZnSe/NiO heterostructure-based chemiresistive-type sensors for low-concentration NO2 detection. Rare Metals, 2021, 40, 1632-1641.	7.1	38
36	Light Activation of Nanocrystalline Metal Oxides for Gas Sensing: Principles, Achievements, Challenges. Nanomaterials, 2021, 11, 892.	4.1	38

#	Article	IF	CITATIONS
37	Influence of copper on sensor properties of tin dioxide films in H2S. Materials Science and Engineering B: Solid-State Materials for Advanced Technology, 1996, 41, 228-234.	3.5	37
38	Materials for solid-state gas sensors. Inorganic Materials, 2000, 36, 293-301.	0.8	37
39	Hydrogen sensitivity of SnO2 thin films doped with Pt by laser ablation. Sensors and Actuators B: Chemical, 2005, 107, 387-391.	7.8	37
40	Role of Pt Aggregates in Pt/SnO[sub 2] Thin Films Used as Gas Sensors Investigations of the Catalytic Effect. Journal of the Electrochemical Society, 2000, 147, 3131.	2.9	36
41	Active Sites on Nanocrystalline Tin Dioxide Surface: Effect of Palladium and Ruthenium Oxides Clusters. Journal of Physical Chemistry C, 2014, 118, 21541-21549.	3.1	35
42	Optical and photoelectrical properties of nanocrystalline indium oxide with small grains. Thin Solid Films, 2015, 595, 25-31.	1.8	33
43	Comparison of Au-functionalized semiconductor metal oxides in sensitivity to VOC. Sensors and Actuators B: Chemical, 2021, 326, 128980.	7.8	33
44	Nanocrystalline tin dioxide: Basics in relation with gas sensing phenomena. Part I. Physical and chemical properties and sensor signal formation. Inorganic Materials, 2015, 51, 1329-1347.	0.8	32
45	Sub-ppm Formaldehyde Detection by n-n TiO2@SnO2 Nanocomposites. Sensors, 2019, 19, 3182.	3.8	32
46	Effect of AuPd Bimetal Sensitization on Gas Sensing Performance of Nanocrystalline SnO2 Obtained by Single Step Flame Spray Pyrolysis. Nanomaterials, 2019, 9, 728.	4.1	31
47	Sub-ppm H2S sensing by tubular ZnO-Co3O4 nanofibers. Sensors and Actuators B: Chemical, 2020, 307, 127624.	7.8	31
48	Doping effects on electrical and optical properties of spin-coated ZnO thin films. Vacuum, 2015, 114, 198-204.	3.5	30
49	Quasi Similar Routes of NO2 and NO Sensing by Nanocrystalline WO3: Evidence by In Situ DRIFT Spectroscopy. Sensors, 2019, 19, 3405.	3.8	30
50	Role of PdO <sub><i>x</i></sub> and RuO <sub><i>y</i></sub> Clusters in Oxygen Exchange between Nanocrystalline Tin Dioxide and the Gas Phase. Journal of Physical Chemistry C, 2013, 117, 23858-23867.	3.1	28
51	Sensor properties of vanadium oxide nanotubes. Mendeleev Communications, 2008, 18, 6-7.	1.6	27
52	Chemically modified nanocrystalline SnO2-based materials for nitrogen-containing gases detection using gas sensor array. Journal of Alloys and Compounds, 2017, 691, 514-523.	5.5	27
53	Gold Decoration and Photoresistive Response to Nitrogen Dioxide of WS <sub>2</sub> Nanotubes. Chemistry - A European Journal, 2018, 24, 18952-18962.	3.3	27
54	Effect of Au and NiO catalysts on the NO2 sensing properties of nanocrystalline SnO2. Inorganic Materials, 2010, 46, 232-236.	0.8	26

#	Article	IF	CITATIONS
55	Gas-sensing behaviors of TiO2-layer-modified SnO2 quantum dots in self-heating mode and effects of the TiO2 layer. Sensors and Actuators B: Chemical, 2020, 310, 127870.	7.8	26
56	Inorganic structures as materials for gas sensors. Russian Chemical Reviews, 2004, 73, 939-956.	6.5	25
57	Photoconductivity of nanocrystalline SnO <sub>2</sub> sensitized with colloidal CdSe quantum dots. Journal of Materials Chemistry C, 2013, 1, 1005-1010.	5.5	25
58	Pyrosol spraying deposition of copper- and nickel-doped tin oxide films. Materials Science and Engineering B: Solid-State Materials for Advanced Technology, 1996, 41, 333-338.	3.5	24
59	Catalytic impact of RuOx clusters to high ammonia sensitivity of tin dioxide. Sensors and Actuators B: Chemical, 2012, 175, 186-193.	7.8	24
60	pH control of the structure, composition, and catalytic activity of sulfated zirconia. Journal of Solid State Chemistry, 2013, 198, 496-505.	2.9	24
61	Effect of Humidity on Light-Activated NO and NO2 Gas Sensing by Hybrid Materials. Nanomaterials, 2020, 10, 915.	4.1	24
62	Photoresistive gas sensor based on nanocrystalline ZnO sensitized with colloidal perovskite CsPbBr3 nanocrystals. Sensors and Actuators B: Chemical, 2021, 329, 129035.	7.8	24
63	CO and NH3 sensor properties and paramagnetic centers of nanocrystalline SnO2 modified by Pd and Ru. Thin Solid Films, 2011, 520, 904-908.	1.8	23
64	Influence of Mono- and Bimetallic PtOx, PdOx, PtPdOx Clusters on CO Sensing by SnO2 Based Gas Sensors. Nanomaterials, 2018, 8, 917.	4.1	22
65	Nanocrystalline LaCoO3 modified by Ag nanoparticles with improved sensitivity to H2S. Sensors and Actuators B: Chemical, 2019, 296, 126661.	7.8	22
66	Nanocomposites SnO2/SiO2 for CO Gas Sensors: Microstructure and Reactivity in the Interaction with the Gas Phase. Materials, 2019, 12, 1096.	2.9	22
67	Two successive effects in the interaction of nanocrystalline SnO2 thin films with reducing gases. Materials Science and Engineering B: Solid-State Materials for Advanced Technology, 2000, 77, 159-166.	3.5	21
68	SnO2/Fe2O3 nanocomposites: Ethanol-sensing performance and catalytic activity for oxidation of ethanol. Inorganic Materials, 2006, 42, 1088-1093.	0.8	21
69	Nanocrystalline ferrites NixZn1â^'xFe2O4: Influence of cation distribution on acidic and gas sensing properties. Journal of Solid State Chemistry, 2011, 184, 2799-2805.	2.9	20
70	p-CoOx/n-SnO2 nanostructures: New highly selective materials for H2S detection. Sensors and Actuators B: Chemical, 2018, 255, 564-571.	7.8	20
71	Selective modified SnO2-based materials for gas sensors arrays. Procedia Chemistry, 2009, 1, 204-207.	0.7	19
72	Cobalt location in p-CoOx/n-SnO2 nanocomposites: Correlation with gas sensor performances. Journal of Alloys and Compounds, 2017, 721, 249-260.	5.5	19

#	Article	IF	CITATIONS
73	Effect of microstructure on the stability of nanocrystalline tin dioxide ceramics. Journal of Materials Chemistry, 1997, 7, 2269-2272.	6.7	18
74	Metal-oxide based nanocomposites as materials for gas sensors. Russian Journal of General Chemistry, 2008, 78, 1081-1092.	0.8	18
75	Active sites on the surface of nanocrystalline semiconductor oxides ZnO and SnO2 and gas sensitivity. Russian Chemical Bulletin, 2017, 66, 1728-1764.	1.5	18
76	Sensitivity of nanocrystalline tungsten oxide to CO and ammonia gas determined by surface catalysts. Sensors and Actuators B: Chemical, 2018, 277, 336-346.	7.8	18
77	Photosensitive Organic-Inorganic Hybrid Materials for Room Temperature Gas Sensor Applications. Nanomaterials, 2018, 8, 671.	4.1	18
78	Room Temperature Formaldehyde Sensing of Hollow SnO <sub>2</sub> /ZnO Heterojunctions Under UV-LED Activation. IEEE Sensors Journal, 2019, 19, 7207-7214.	4.7	18
79	Ga2O3(Sn) Oxides for High-Temperature Gas Sensors. Nanomaterials, 2021, 11, 2938.	4.1	18
80	Mass Spectrometric Study of Nanocrystalline ZnO Vaporization. Inorganic Materials, 2003, 39, 594-598.	0.8	17
81	Influence of the microstructure of semiconductor sensor materials on oxygen chemisorption on their surface. Russian Journal of General Chemistry, 2008, 78, 2556-2565.	0.8	17
82	Specific Interaction of PdO <sub><i>x</i></sub> - and RuO <sub><i>y</i></sub> -Modified Tin Dioxide with CO and NH <sub>3</sub> Gases: Kelvin Probe and DRIFT Studies. Journal of Physical Chemistry C, 2015, 119, 24342-24350.	3.1	17
83	Effects of Ag Additive in Low Temperature CO Detection with In2O3 Based Gas Sensors. Nanomaterials, 2018, 8, 801.	4.1	17
84	Hydrothermal Synthesis of Nanocrystalline SnO2 for Gas Sensors. Inorganic Materials, 2003, 39, 1158-1162.	0.8	16
85	Pd nanoparticles on SnO2(Sb) whiskers: Aggregation and reactivity in CO detection. Journal of Alloys and Compounds, 2013, 565, 6-10.	5.5	16
86	Selectivity of Catalytically Modified Tin Dioxide to CO and NH3 Gas Mixtures. Chemosensors, 2015, 3, 241-252.	3.6	16
87	Synergy Effect of Au and SiO2 Modification on SnO2 Sensor Properties in VOCs Detection in Humid Air. Nanomaterials, 2020, 10, 813.	4.1	16
88	Impedance spectroscopy of ultrafine-grain SnO2 ceramics with a variable grain size. Semiconductors, 2006, 40, 104-107.	0.5	15
89	Charge carrier transport mechanisms in nanocrystalline indium oxide. Thin Solid Films, 2014, 558, 320-325.	1.8	15
90	Highly Sensitive ZnO(Ga, In) for Sub-ppm Level NO2 Detection: Effect of Indium Content. Chemosensors, 2017, 5, 18.	3.6	15

#	Article	IF	CITATIONS
91	Light-Activated Sub-ppm NO2 Detection by Hybrid ZnO/QD Nanomaterials vs. Charge Localization in Core-Shell QD. Frontiers in Materials, 2019, 6, .	2.4	15
92	The electrical conductivity of polycrystalline SnO2(Cu) films and their sensitivity to hydrogen sulfide. Semiconductors, 1997, 31, 335-339.	0.5	14
93	Crystallite size effect on the conductivity of the ultradisperse ceramics of SnO2 and In2O3. Mendeleev Communications, 2004, 14, 167-169.	1.6	14
94	Materials based on modified SnO2 for selective gas sensors. Inorganic Materials, 2010, 46, 1100-1105.	0.8	14
95	Conductivity of nanocrystalline ZnO(Ga). Semiconductors, 2013, 47, 650-654.	0.5	14
96	High-temperature resistive gas sensors based on ZnO/SiC nanocomposites. Beilstein Journal of Nanotechnology, 2019, 10, 1537-1547.	2.8	14
97	Electrospun ZnO/Pd Nanofibers: CO Sensing and Humidity Effect. Sensors, 2020, 20, 7333.	3.8	14
98	Acidic and catalytic co-functionalization for tuning the sensitivity of sulfated tin oxide modified by ruthenium oxide to ammonia gas. Sensors and Actuators B: Chemical, 2018, 255, 3523-3532.	7.8	13
99	Determination of gold and cobalt dopants in advanced materials based on tin oxide by slurry sampling high-resolution continuum source graphite furnace atomic absorption spectrometry. Spectrochimica Acta, Part B: Atomic Spectroscopy, 2018, 140, 1-4.	2.9	13
100	Effect of Zinc Oxide Modification by Indium Oxide on Microstructure, Adsorbed Surface Species, and Sensitivity to CO. Frontiers in Materials, 2019, 6, .	2.4	13
101	Unusual distribution of the constituents of an (Fe2O3)0.8(SnO2)0.2 nanocomposite evidenced by 57Fe and 119Sn Mössbauer spectroscopy. Mendeleev Communications, 2004, 14, 140-141.	1.6	12
102	Synthesis, microstructure, and gas-sensing properties of SnO2/MoO3 nanocomposites. Inorganic Materials, 2005, 41, 370-377.	0.8	12
103	Charge carrier transport in indium oxide nanocrystals. Journal of Experimental and Theoretical Physics, 2010, 111, 653-658.	0.9	12
104	Microstructure and gas-sensing properties of nanocrystalline NiFe2O4 prepared by spray pyrolysis. Inorganic Materials, 2010, 46, 1254-1259.	0.8	12
105	The Effect of CdSe and InP Quantum Dots on the Interaction of ZnO with NO2 under Visible Light Irradiation. Russian Journal of Inorganic Chemistry, 2018, 63, 512-518.	1.3	12
106	Effect of W‒O bonding on gas sensitivity of nanocrystalline Bi2WO6 and WO3. Journal of Alloys and Compounds, 2021, 856, 158159.	5.5	12
107	Sensor Properties of Pd-Doped SnO2 Films Deposited by Laser Ablation. Inorganic Materials, 2002, 38, 374-379.	0.8	11
108	Metal Oxide Nanocomposites: Synthesis and Characterization in Relation with Gas Sensing Phenomena. NATO Science for Peace and Security Series C: Environmental Security, 2009, , 3-30.	0.2	11

#	Article	IF	CITATIONS
109	EPR study of nanocrystalline tin dioxide. Physica Status Solidi C: Current Topics in Solid State Physics, 2011, 8, 1957-1960.	0.8	11
110	Hybrid sensor materials based on tin(IV) oxide and crown-containing 4-amino-1,8-naphthalimides. Mendeleev Communications, 2011, 21, 12-14.	1.6	11
111	Pulsed laser deposition of conductive indium tin oxide thin films. Inorganic Materials, 2012, 48, 1020-1025.	0.8	11
112	Cation distribution in nanocrystalline Ni x Zn1 â^' x Fe2O4 spinel ferrites. Inorganic Materials, 2012, 48, 525-530.	0.8	11
113	Organic-Inorganic Hybrid Materials for Room Temperature Light-Activated Sub-ppm NO Detection. Nanomaterials, 2020, 10, 70.	4.1	11
114	UV-Activated NO2 Gas Sensing by Nanocrystalline ZnO: Mechanistic Insights from Mass Spectrometry Investigations. Chemosensors, 2022, 10, 147.	3.6	11
115	Physicochemical properties of fine-particle ZnFe2O4 prepared by spray pyrolysis of nitrate solutions. Inorganic Materials, 2007, 43, 853-859.	0.8	10
116	Influence of antimony doping on structure and conductivity of tin oxide whiskers. Thin Solid Films, 2009, 518, 1359-1362.	1.8	10
117	Inversion of NH3 sensor signal and paramagnetic centers of nanocrystalline ZnO(Ga). Procedia Engineering, 2011, 25, 296-299.	1.2	10
118	Photoconductivity of structures based on the SnO <sub>2</sub> porous matrix coupled with core-shell CdSe/CdS quantum dots. Applied Physics Letters, 2013, 103, 133115.	3.3	10
119	The acetic acid vapor sensing properties of BaSnO3 microtubes prepared by electrospinning method. Materials Science and Engineering B: Solid-State Materials for Advanced Technology, 2020, 259, 114606.	3.5	10
120	High-Sensitivity Humidity Sensor Based on a Single Sb-Doped SnO <sub>2</sub> Whisker. Sensor Letters, 2009, 7, 1025-1029.	0.4	10
121	Crystalline WO3 nanoparticles for No2 sensing. Processing and Application of Ceramics, 2020, 14, 282-292.	0.8	10
122	Design, Synthesis and Application of Metal Oxide-Based Sensing Elements: A Chemical Principles Approach. , 2013, , 69-115.		9
123	Ultrasonic disintegration of tungsten trioxide pseudomorphs after ammonium paratungstate as a route for stable aqueous sols of nanocrystalline WO3. Journal of Materials Science, 2018, 53, 1758-1768.	3.7	9
124	Enhancement of Lewis Acidity of Crâ€Doped Nanocrystalline SnO <sub>2</sub> : Effect on Surface NH <sub>3</sub> Oxidation and Sensory Detection Pattern. ChemPhysChem, 2019, 20, 1985-1996.	2.1	9
125	p-n Transition-Enhanced Sensing Properties of rGO-SnO <sub>2</sub> Heterojunction to NO <sub>2</sub> at Room Temperature. IEEE Sensors Journal, 2020, 20, 4562-4570.	4.7	9
126	Microstructure and sensing properties of nanocrystalline indium oxide prepared using hydrothermal treatment. Russian Journal of Inorganic Chemistry, 2009, 54, 163-171.	1.3	8

#	Article	IF	CITATIONS
127	Antimony doped whiskers of SnO2 grown from vapor phase. Journal of Crystal Growth, 2010, 312, 386-390.	1.5	8
128	Nanocrystalline tin dioxide: Basics in relation with gas sensing phenomena part II. Active centers and sensor behavior. Inorganic Materials, 2016, 52, 1311-1338.	0.8	8
129	Quantification of modifiers in advanced materials based on zinc oxide by total reflection X-ray fluorescence and inductively coupled plasma mass spectrometry. Spectrochimica Acta, Part B: Atomic Spectroscopy, 2016, 118, 62-65.	2.9	8
130	Effect of Bimetallic Pd/Pt Clusters on the Sensing Properties of Nanocrystalline SnO2 in the Detection of CO. Russian Journal of Inorganic Chemistry, 2018, 63, 1007-1011.	1.3	8
131	First-principles study of CO and OH adsorption on in-doped ZnO surfaces. Journal of Physics and Chemistry of Solids, 2019, 132, 172-181.	4.0	8
132	Nanocomposites SnO2/SiO2:SiO2 Impact on the Active Centers and Conductivity Mechanism. Materials, 2019, 12, 3618.	2.9	8
133	Influence of In <sub>2</sub> O <sub>3</sub> Nanocrystals Size on the Sensitivity to NO <sub>2</sub> . Journal of Nanoelectronics and Optoelectronics, 2011, 6, 452-455.	0.5	8
134	Au Functionalized SnS2 Nanosheets Based Chemiresistive NO2 Sensors. Chemosensors, 2022, 10, 165.	3.6	8
135	Memory effect and its switching by electric field in solid-state gas sensors. Materials Science and Engineering B: Solid-State Materials for Advanced Technology, 2000, 77, 106-109.	3.5	7
136	Vapor growth of SnO2 whiskers. Inorganic Materials, 2007, 43, 964-967.	0.8	7
137	Effect of oxygen partial pressure on SnO2 whisker growth. Inorganic Materials, 2008, 44, 268-271.	0.8	7
138	H2S Sensing by Hybrids Based on Nanocrystalline SnO2 Functionalized with Cu(II) Organometallic Complexes: The Role of the Ligand Platform. Nanomaterials, 2017, 7, 384.	4.1	7
139	Nanocrystalline complex oxides NixCo3-xO4: Cations distribution impact on electrical and gas sensor behaviour. Journal of Alloys and Compounds, 2020, 828, 154420.	5.5	7
140	Conductivity of ultradispersed SnO2 ceramic in strong electric fields. Semiconductors, 2009, 43, 156-157.	0.5	6
141	Frequency-dependent electrical conductivity of nanocrystalline SnO2. Inorganic Materials, 2013, 49, 1000-1004.	0.8	6
142	SnO2(Au0, Coll, III) nanocomposites: A synergistic effect of the modifiers in CO detection. Inorganic Materials, 2016, 52, 94-100.	0.8	6
143	Nanocrystalline Oxides NixCo3â^'xO4: Sub-ppm H2S Sensing and Humidity Effect. Chemosensors, 2021, 9, 34.	3.6	6
144	UV-VIS Photoconductivity of Nanocrystalline Tin Oxide. Journal of Nanoelectronics and Optoelectronics, 2012, 7, 623-628.	0.5	6

#	Article	IF	CITATIONS
145	In2O3 Based Hybrid Materials: Interplay between Microstructure, Photoelectrical and Light Activated NO2 Sensor Properties. Chemosensors, 2022, 10, 135.	3.6	6
146	Copper diffusion in SnO2 polycrystalline films. Journal of Materials Science Letters, 1994, 13, 1632-1634.	0.5	5
147	Conductivity of structures based on doped nanocrystalline SnO2 films with gold contacts. Semiconductors, 1999, 33, 175-176.	0.5	5
148	Properties of diode heterostructures based on nanocrystalline n-SnO2 on p-Si under the conditions of gas Adsorption. Semiconductors, 2000, 34, 955-959.	0.5	5
149	Effect of heterovalent substitution on the electrical and optical properties of ZnO(M) thin films (M =) Tj ETQq1 1	0.784314	rgBT /Over
150	Effect of n -type Doping of SnO 2 and ZnO on Surface Sites and Gas Sensing Behaviour. Procedia Engineering, 2016, 168, 1082-1085.	1.2	5
151	Detection of Carbon Monoxide in Humid Air with Double-Layer Structures Based on Semiconducting Metal Oxides and Silicalite. Russian Journal of Applied Chemistry, 2018, 91, 1671-1679.	0.5	5
152	Tin oxide nanomaterials: Active centers and gas sensor properties. , 2020, , 163-218.		5
153	Electron injection effect in In <sub>2</sub> O <sub>3</sub> and SnO <sub>2</sub> nanocrystals modified by ruthenium heteroleptic complexes. Physical Chemistry Chemical Physics, 2020, 22, 8146-8156.	2.8	5
154	Simple in situ analysis of metal halide perovskite-based sensor materials using micro X-ray fluorescence and inductively coupled plasma mass spectrometry. Mendeleev Communications, 2021, 31, 462-464.	1.6	5
155	Low Temperature HCHO Detection by SnO2/TiO2@Au and SnO2/TiO2@Pt: Understanding by In-Situ DRIFT Spectroscopy. Nanomaterials, 2021, 11, 2049.	4.1	5
156	Nanocrystalline SnO2 Functionalized with Ag(I) Organometallic Complexes as Materials for Low Temperature H2S Detection. Materials, 2021, 14, 7778.	2.9	5
157	Effect of doping metals on the kinetics of interaction of SnO2 thin films with oxygen. Journal of Materials Chemistry, 1998, 8, 1577-1581.	6.7	4
158	Electrical Properties of Nanocrystalline n-SnO2 to Single Crystal p-Si Interfaces under Gas Adsorption Conditions. Physica Status Solidi A, 2001, 188, 1093-1104.	1.7	4
159	Kinetics of Interaction of Thick Nanocrystalline SnO <sub>2</sub> Films with Oxygen. Inorganic Materials, 2004, 40, 161-165.	0.8	4
160	Effect of the conditions of structure formation on the physicochemical properties of ozonated shungites. Russian Journal of Physical Chemistry A, 2010, 84, 1376-1381.	0.6	4
161	Determination of antimony and tin in tin dioxide whiskers by inductively coupled plasma mass spectrometry. Journal of Analytical Chemistry, 2012, 67, 950-954.	0.9	4
162	Photoconductivity of composite structures based on porous SnO2 sensitized with CdSe nanocrystals. Semiconductors, 2013, 47, 383-386.	0.5	4

#	Article	IF	CITATIONS
163	Voltage effect on the sensitivity of nanocrystalline indium oxide to nitrogen dioxide under ultraviolet irradiation. Technical Physics Letters, 2015, 41, 252-254.	0.7	4
164	Determination of selenium and cadmium dopants in nanocomposites based on zinc and indium oxides by high resolution continuous source electrothermal atomic absorption spectrometry and inductively coupled plasma mass spectrometry. Journal of Analytical Chemistry, 2016, 71, 496-499.	0.9	4
165	Effect of Ga and in doping on acid centers and oxygen chemisorption on the surface of nanocrystalline ZnO. Inorganic Materials, 2016, 52, 578-583.	0.8	4
166	Nanocrystalline Metal Oxides as Promising Materials for Gas Sensors for Hydrogen Sulfide. Russian Journal of Applied Chemistry, 2001, 74, 434-439.	0.5	3
167	Optical and photoelectric properties of nanocrystalline SnO <sub>2</sub> ―CdSe quantum dot structures. Physica Status Solidi C: Current Topics in Solid State Physics, 2010, 7, 972-975.	0.8	3
168	Acetone Sensing by Modified SnO2 Nanocrystalline Sensor Materials. NATO Science for Peace and Security Series B: Physics and Biophysics, 2011, , 409-421.	0.3	3
169	Catalytic impact of RuOx clusters to high NH3 sensitivity of tin dioxide. Procedia Engineering, 2011, 25, 227-230.	1.2	3
170	Transport properties of thin SnO2〈Sb〉 films grown by pulsed laser deposition. Inorganic Materials, 2013, 49, 1123-1126.	0.8	3
171	The optoelectronic properties of nitrogen- and carbon-doped nanocrystalline titania. Moscow University Physics Bulletin (English Translation of Vestnik Moskovskogo Universiteta, Fizika), 2013, 68, 387-396.	0.4	3
172	Analysis of CO and NH <sub>3</sub> Reductive Gases Mixture by Chemically Modified Nanocrystalline Tin Dioxide. Key Engineering Materials, 0, 605, 227-230.	0.4	3
173	Effect of cadmium-selenide quantum dots on the conductivity and photoconductivity of nanocrystalline indium oxide. Semiconductors, 2016, 50, 607-611.	0.5	3
174	Cooperative effect of PdOx and SiO2 in CO detection by SnO2-based gas sensors: Thorough operando DRIFTS analysis. Journal of Alloys and Compounds, 2022, 893, 162297.	5.5	3
175	Pre-concentration of organophosphorous compounds on porous silica materials. Studies in Surface Science and Catalysis, 2008, 174, 623-626.	1.5	2
176	Kinetics of interaction between nanocrystalline SnO2〈M〉 (M = In, Fe, Ru, Ce) and oxygen. Inorganic Materials, 2009, 45, 1153-1157.	0.8	2
177	Effect of surface modification with palladium on the CO sensing properties of antimony-doped SnO2 whiskers. Inorganic Materials, 2013, 49, 1005-1010.	0.8	2
178	Controlling the phase composition of cadmium sulfide films during pulsed laser deposition. Inorganic Materials, 2017, 53, 1120-1125.	0.8	2
179	High Temperature Resistive Gas Sensors Based on ZnO/SiC Nanocomposites. Proceedings (mdpi), 2019, 14, 36.	0.2	2
180	Effect of WO3 particle size on the type and concentration of surface oxygen. Mendeleev Communications, 2020, 30, 126-128.	1.6	2

#	Article	IF	CITATIONS
181	Synthesis, Optical Characteristics and Complex Formation of Molecular Receptors Based on 1,8-Naphthalimide Derivatives in Solution and in Composition of Hybrid Tin Dioxide Nanoparticles. Macroheterocycles, 2017, 10, 84-93.	0.5	2
182	Flame-Made La2O3-Based Nanocomposite CO2 Sensors as Perspective Part of GHG Monitoring System. Sensors, 2021, 21, 7297.	3.8	2
183	Nanocrystalline Complex Oxides Zn <i><sub>x</sub></i> Co <sub>3–<i>x</i></sub> O <sub>4</sub> : Cobalt and Zinc Ions Impact on Large Growth of Conductivity. Journal of Physical Chemistry C, 0, , .	3.1	2
184	Influence of the boundary on the interdiffusion in heterostructures. Materials Science and Engineering B: Solid-State Materials for Advanced Technology, 1994, 26, 147-149.	3.5	1
185	Electric-field-controlled memory effect in heterostructures for gas sensors. Technical Physics Letters, 1999, 25, 471-474.	0.7	1
186	Interface states and capacitance-voltage characteristics of n-SnO2:Ni/p-Si heterostructures under gas-adsorption conditions. Semiconductors, 2001, 35, 424-426.	0.5	1
187	Fe2O3:SnO2 Nanostructured System as Semiconductor Gas Sensor Material. Materials Research Society Symposia Proceedings, 2004, 828, 215.	0.1	1
188	Influence of La(III) on the reactivity and sensor properties of nanocrystalline SnO2. Russian Journal of Inorganic Chemistry, 2016, 61, 1368-1373.	1.3	1
189	Effect of antimony on the reaction of nanocrystalline SnO2 with oxygen. Inorganic Materials, 2016, 52, 1-6.	0.8	1
190	Light—Assisted Low Temperature Formaldehyde Detection at Sub-ppm Level Using Metal Oxide Semiconductor Gas Sensors. Proceedings (mdpi), 2019, 14, 37.	0.2	1
191	ZnSe/NiO heterostructure-based chemiresistive-type sensors for low-concentration NO2 detection. , 0, .		1
192	Study of the Reactivity of Nanocrystallites of SnO2 With H2S by Coupled Electrical and Raman Measurements. , 1999, , 285-290.		1
193	Physicochemical and functional peculiarities of metal oxide whiskers. Russian Chemical Bulletin, 2008, 57, 1042-1053.	1.5	0
194	Sensor properties of hybrid SnO2-polysilazane materials. Procedia Chemistry, 2009, 1, 172-175.	0.7	0
195	Synthesis, surface modification and ethanol sensing properties of Sb-doped SnO 2. Proceedings of SPIE, 2009, , .	0.8	0
196	Detection of organophosphorus compounds with semiconductor gas sensors using adsorption preconcentration. Russian Journal of Applied Chemistry, 2013, 86, 1682-1690.	0.5	0
197	Combination of tailored acid-base and red/ox properties of nanocrystalline SnO <inf>2</inf> for optimal gas sensor performance: Principle applicability study on NH <inf>3</inf> and H <inf>2</inf> S examples. , 2013, , .		0
198	Interplay between active sites of modified nanocrystalline tin dioxide and selectivity to CO and NH <inf>3</inf> gases. , 2014, , .		0

#	Article	IF	CITATIONS
199	Effect of the tin impurity on the energy spectrum and photoelectric properties of nanostructured In2O3 films. Semiconductors, 2014, 48, 451-454.	0.5	0
200	Synthesis of ZnO Thin Films Doped with Ga and In: Determination of Their Composition through X-Ray Spectroscopy and Inductively Coupled Plasma Mass Spectrometry. Inorganic Materials, 2017, 53, 1458-1462.	0.8	0
201	Nanocrystalline LaCoO3 Modified by Ag Nanoparticles with Improved Sensitivity to H2S. Proceedings (mdpi), 2019, 14, 44.	0.2	0
202	WS2 nanotubes dressed in gold and silver: Synthesis, optoelectronic properties, and NO2 sensing. AIP Conference Proceedings, 2021, , .	0.4	0
203	Obituary for Prof. Dr. Alexander Gaskov. Sensors, 2021, 21, 2913.	3.8	0
204	Structural and Optoelectronic Properties of Tin Oxide Nanocrystals Prepared by Wet Chemistry Methods. Journal of Nanoelectronics and Optoelectronics, 2011, 6, 514-518.	0.5	0
205	SnO <sub>2</sub> Whiskers with Pd Nanoparticles for Gas Sensor Applications. Journal of Nanoelectronics and Optoelectronics. 2012. 7. 607-613.	0.5	0